Modelling of high-field-side high-density region with the nonlinear MHD code JOREK with kinetic neutrals

S.Q. Korving[1,2], G.T.A. Huijsmans[1,3], J.-S. Park[4], and the JOREK team (see ref [1])

[1] *Eindhoven University of Technology , Eindhoven, The Netherlands*

[2] *ITER Organization, St. Paul Lez Durance Cedex, France*

[3] *CEA, IRFM, St. Paul Lez Durance Cedex, France*

[4] *Korea Advanced Institute of Technology, Daejeon 34141, Republic of Korea*

It has been shown that controlling the X-point radiator in a fully detached H-mode plasma can lead to a naturally more ELM-stable regime [3]. This might become an important strategy in heat load-, and ELM-control. Precursing the X-point radiator is the HFSHD-region (High-Field-Side High-Density region). Poloidal $\overrightarrow{E}\times\overrightarrow{B}$ flows below the X-point redistribute part of the main plasma from the outer to inner divertor; this aides the onset of inner target (IT) detachment [5]. Once the IT partially detaches, a high-field-side (HFS) $\overrightarrow{E}\times\overrightarrow{B}$ vortex increasingly transports density upwards and leads to the formation of the HFSHD-region. The nonlinear extended MHD code JOREK [1, 2] has recently been extended with a module for kinetic neutrals and more plasma and neutral wall interaction physics. With this addition, JOREK has been successfully benchmarked against SOLPS-ITER simulations for fueling-driven detachment in ITER PFPO-1 [6]. It also allows for the simulation of the HFSHD-region. In this contribution, we present a benchmark of the kinetic neutrals, the onset of detachment and the formation of the HFSHD-region in JOREK.

Fluid MHD plus kinetic neutral physics in JOREK

JOREK is a fully implicit non-linear extended MHD code for realistic tokamak X-point plasmas [1, 2]. Here, the visco-resistive reduced MHD is used as model where the time-evolved parameters are ψ, j, u, ω, ρ, $T = T_i + T_e$, $v_{\|}$, respectively the poloidal flux, the toroidal current density, the poloidal velocity stream function, the vorticity, the mass density, the ion plus electron temperature and the parallel velocity. The JOREK MHD model has been extended with a Monte-Carlo kinetic particle code [4]. The kinetic neutrals consist of super-particles with a weight (i.e. the amount of physical particles), a position and velocity in three dimensions. The physical coupling to the plasma is via ionisation, recombination, charge-exchange (CX) and recycling at the wall. The line-radiation, recombination radiation and Bremsstrahlung losses are included as well. To add these sources/sinks to the fluid equations, moments of the discrete particle distribution need to be converted to a continuous—in space—description of the finite element basis. This is done by equating the list of discrete particle moments with a continuous function. The resulting set of equations [1] depend only on the finite element geometry. The lhs of the system of equations needs to be factorized only once. The system needs to be solved at every fluid time step.

SOLPS-ITER comparison for PFPO-1 H-mode plasmas without poloidal flows.

To test the implementation of the neutrals code development, JOREK simulations are compared to SOLPS-ITER simulations of an ITER (Pre Fusion Power Operation) PFPO-1 H-mode scenario without impurities [6]. Here the simulations are performed for a range of different neutral fueling rates in the divertor. The details of the scenario are $B_T = 1.85$ T, $I_p = 5$MA, $P_{heating} = 20$ MW, $D_\perp = 0.3$ $\mathrm{m^2 s^{-1}}$, $\chi_{i,\perp} = \chi_{e,\perp} = 1.0$ $\mathrm{m^2 s^{-1}}$. Parallel heat transport is based on the Braginskii closure.

SOLPS-ITER does not resolve the plasma core nor evolves the magnetic equilibrium. To obtain the self-consistent equilibrium close to the SOLPS-ITER solution, as required by JOREK, we take the pressure profile from the EQDSK equilibrium on which the SOLPS-ITER runs are based. To reach a quasi-steady-state JOREK simulation were run ~ 42 ms.

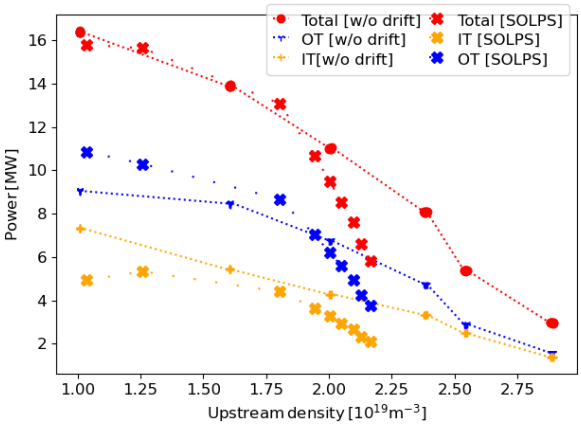

Figure 1: *The inner, outer, and total divertor heat load as function of the outer midplane separatrix electron density (n_u) for SOLPS-ITER [SOLPS] and JOREK with kinetic neutrals [w/o drift]. All results in this figure are without drifts.*

To reduce the set of time-evolved physics, i.e. removing poloidal flows, to be consistent with the SOLPS-ITER physics model, we have removed the time evolution of ψ, j, u, ω in these benchmark simulations. The reduced model is the closest to SOLPS-ITER without drifts. Only the results without drifts are directly comparable between JOREK and SOLPS-ITER. Here, we only look at the total plasma heat load to the divertor as function as the upstream density (n_u) as a global overview.

At the lower- to mid-range of the upstream density ($n_u \lesssim 2{\times}10^{19}\text{m}^{-3}$), there is good agreement in total power of JOREK with SOLPS-ITER. The inner-outer divertor power balance is slightly more symmetric than SOLPS-ITER. Beyond $n_u \approx 2{\times}10^{19}\text{m}^{-3}$, the SOLPS-ITER plasma transitions from high-recycling to a fully detached divertor plasma. While this happens n_u starts to saturate. In the no-drift JOREK simulation, the transition to detachment occurs at about 10% higher n_u than SOLPS-ITER. The transition as function of n_u is less sharp in JOREK. The slope ($\partial Power/\partial n_u$) is decreasing for higher n_u. This does indicate a similar but less strong form of density saturation from $n_u \gtrapprox 2.4{\times}10^{19}\text{m}^{-3}$. As our kinetic neutral model now only consists of atoms (i.e. no molecules), and neutral-neutral collisions are neglected, one can expect the comparison with SOLPS-ITER to diverge when detaching the plasma from the divertor.

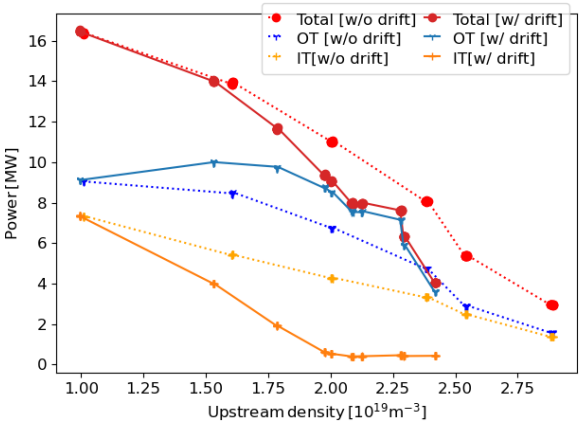

Figure 2: *The inner, outer, and total divertor heat load as function of the outer midplane separatrix electron density (n_u) for JOREK without drifts [w/o drift] and with drift [w/ drift].*

When using the standard JOREK model—which naturally includes $\vec{E}\times\vec{B}$ flows—the total power stays almost the same for $n_u \lesssim 1.6{\times}10^{19}\text{m}^{-3}$; but relatively more power goes towards the outer target (OT) as shown in figure 2. Beyond $n_u \approx 1.6{\times}10^{19}\text{m}^{-3}$, the drifts cause a more sharp saturation into the detached regime. Beyond $n_u \approx 2{\times}10^{19}\text{m}^{-3}$ a phase-like transition occurs. After the transition we ob-

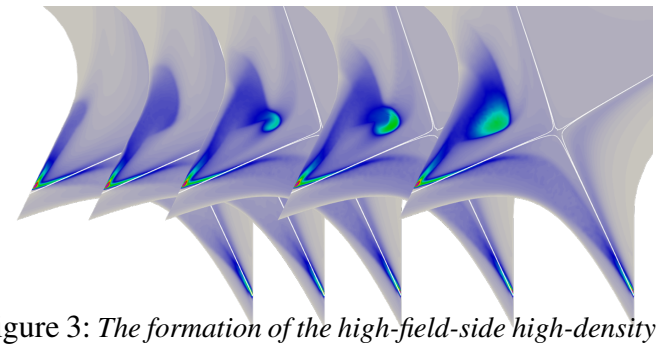

Figure 3: *The formation of the high-field-side high-density region presented as a series of the 2D electron density profiles in the poloidal plane. Note, due to the $\vec{E}\times\vec{B}$ vortex, the precursor and HFSHD-region rotate as well. Thus it does not solely moves in- and outwards.*

serve a stronger upstream density saturation than without the $\overrightarrow{E}\times\overrightarrow{B}$ drifts.

Formation of the High-field-side high-density region

The transition towards a dominant high-field-side (HFS) $\overrightarrow{E}\times\overrightarrow{B}$ vortex and the HFSHD-region is a rather dynamic phenomenon. This transition is shown as a series of five 2D n_e profiles in figure 3. There is an initial slow buildup phase of density close to the wall. This phase is followed by a density front building up, moving from the wall towards the X-point. The $\overrightarrow{E}\times\overrightarrow{B}$ vortex is significant enough to move this high density front. Once the front is close to the X-point, it quickly builds up more and more density, until $n_e \approx 1\times10^{21}$ m^{-3}. It then reaches a critical point the the high density region close the X-point suddenly moves away from the X-point and installs itself at the stable location as shown in the last profile in figure 3 and also in figure 5. Especially during this fast movement away from the X-point, the flow patterns everywhere are altered. Most notably on the HFS of the divertor, but also on the OT and the entire SOL. Figure 4 shows the dynamic ion flux profiles on the IT over a range of n_u. Due to $\overrightarrow{E}\times\overrightarrow{B}$ drifts we observe an early rollover of the ion flux. Due to the flow redistribution of the HFS $\overrightarrow{E}\times\overrightarrow{B}$ vortex, the IT re-attaches with the peak at a different location. Continuing to increase n_u again detaches the plasma at the IT.

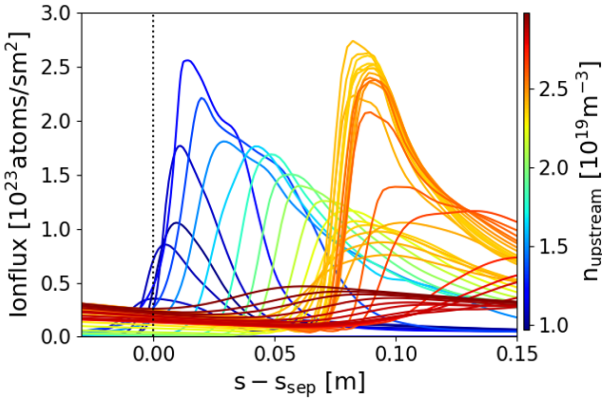

Figure 4: *The progression of the ion flux radially along the inner target. The line colors indicate the upstream density.*

The exact equilibrium position on which the HFSHD-region settles depends on the gas fueling rate in the divertor. Altering the gas fueling rate results in horizontal motion. Exactly how this relation works is not yet fully understood in our simulations.

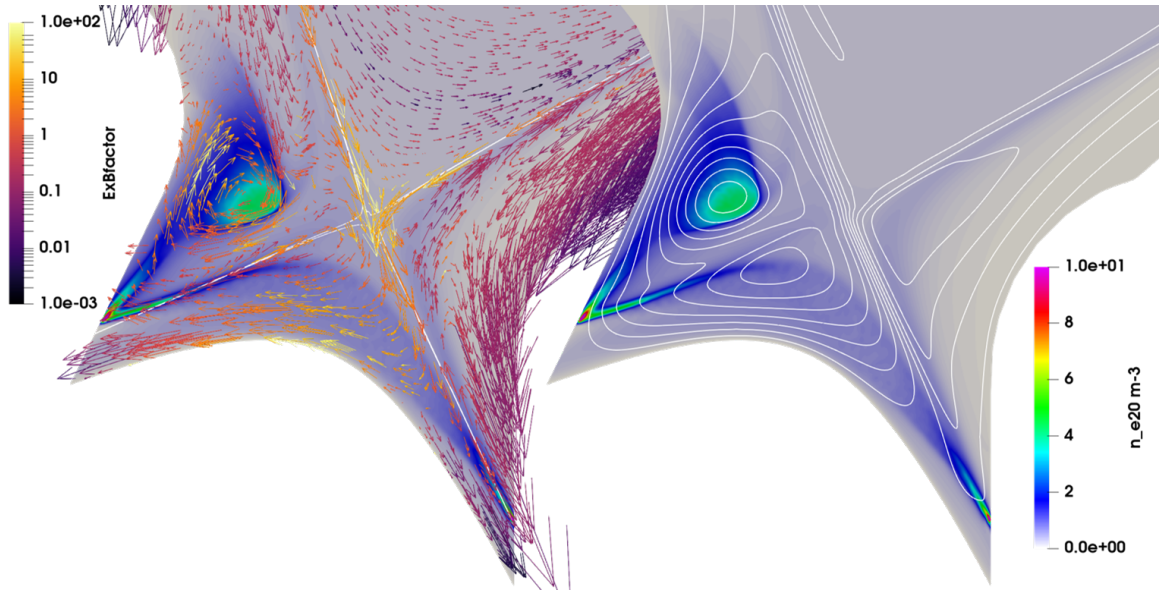

Figure 5: *2D electron density profiles for a detached case for ITER PFPO-1. (left) 2D poloidal flows visualized on top of the 2D electron density profile. The color of the quivers show the importance of the $\overrightarrow{E}\times\overrightarrow{B}$ term. The importance is here defined as* $ExB_{factor} \equiv \frac{|\mathbf{v}_{ExB}|}{|\mathbf{v}_{pol}-\mathbf{v}_{ExB}|} = \frac{|\mathbf{v}_{ExB}|}{|(\mathbf{e}_\phi\times\mathbf{v}_{||})\times\mathbf{e}_\phi|}$*; the magnitude of the $\overrightarrow{E}\times\overrightarrow{B}$ velocity divided by the magnitude of poloidal velocities excluding the $\overrightarrow{E}\times\overrightarrow{B}$ velocity. The thin white line is the separatrix.(right) Electric potential contour on top of the electron density profile. $\overrightarrow{E}\times\overrightarrow{B}$ drifts are along the potential contour lines.*

Figure 5 shows the detached scenario with a fully formed HFSHD-region. It shows the density profile with the poloidal flow vectors colored with the ExB_{factor} on figure 5(left) and the electric potential contours on figure 5(right). Especially the HFS $\overrightarrow{E}\times\overrightarrow{B}$ vortex has grown to become dominant as the $ExB_{factor} \gg 1$. The HFS $\overrightarrow{E}\times\overrightarrow{B}$ vortex draws in plasma density from the IT and it becomes trapped in the vortex. Once the HFSHD-region is stabilized the electric potential forms a plateau where the density is highest. The potential contour patterns already show $\overrightarrow{E}\times\overrightarrow{B}$ vortices in the when the plasma is attached; these features become exaggerated towards detachment. The low-field-side (LFS) $\overrightarrow{E}\times\overrightarrow{B}$ vortex is inferior and does not create a vortex flow pattern. The private region $\overrightarrow{E}\times\overrightarrow{B}$ vortex contributes to enhanced transport from the X-point towards the OT and decreases transport from the X-point to the IT. The private region $\overrightarrow{E}\times\overrightarrow{B}$ vortex is the dominant actor in transporting the plasma from the OT to the IT via the private region.

Summary

In this contribution, we have presented a benchmark of JOREK—without drifts—with kinetic neutrals against SOLPS-ITER (without drifts) and the development of the HFSHD-region in JOREK simulations with kinetic neutrals for early ITER operation (the PFPO-1 phase).

Ramping up the fueling rate (in the divertor) decreases gradually the heat flux towards the divertor target. Once the ionisation front comes off the wall, cross field transport moves neutrals and plasma across the separatrix. Building up the (off-separatrix) density in the high field side. Around a critical upstream density, the plasma undergoes a sharp transition to form the HFSHD-region carried by the formation of an $\overrightarrow{E}\times\overrightarrow{B}$ vortex. This $\overrightarrow{E}\times\overrightarrow{B}$ vortex increases in strength and displaces the inner target ion flux upwards. Switching off $\overrightarrow{E}\times\overrightarrow{B}$ drifts strongly reduces cross-field transport and thus does not allow for the density buildup at the high-field-side. With more accurate divertor solution, JOREK can now better study the consequences in the divertor as a result of MHD instabilities, such as ELMs.

Acknowledgements

This work is part of the research programme of the Foundation for Nederlandse Wetenschappelijk Onderzoek Instituten (NWO-I), which is part of the NWO and has been carried out within the framework of the EUROfusion Consortium, funded by the European Union via the Euratom Research and Training Programme (Grant Agreement No 101052200 — EUROfusion) and by the ITER Organization under Implementing Agreement 43-2174 with the Eindhoven University of Technology. The views and opinions expressed herein do not necessarily reflect those of NWO, the European Commission nor the ITER Organization.

References

[1] M.Hoelzl et al., Nuclear Fusion 61 (2021)
[2] G.T.A. Huijsmans, O. Czarny, Nuclear Fusion 47 (2007)
[3] M. Bernert et al.,IAEA FEC (2020)
[4] D.C van Vugt, PhD thesis, Eindhoven University of Technology, (2019)
[5] V. Rozhansky et al., Nucl. Fusion 61 126073 (2021)
[6] J.-S. Park et al., Nuclear fusion 61, (2021)